



## SPECIAL ISSUE: Flexible Intelligent Materials

# Stable and low-resistance polydopamine methacrylamide-polyacrylamide hydrogel for brain-computer interface

Lanlan Liu<sup>1</sup>, Yafeng Liu<sup>4</sup>, Ruitao Tang<sup>1</sup>, Jun Ai<sup>1</sup>, Yinji Ma<sup>2</sup>, Ying Chen<sup>1,3\*</sup> and Xue Feng<sup>2\*</sup>

**ABSTRACT** Signal drift and performance instability of brain-computer interface devices induced by the interface failure between rigid metal electrodes and soft human skin hinder the precise data acquisition of electroencephalogram (EEG). Thus, it is desirable to achieve a robust interface for brain-computer interface devices. Here, a kind of polydopamine methacrylamide-polyacrylamide (PDMA-PAAM) hydrogel is developed. To improve the adhesion, dopamine is introduced into the polyacrylamide hydrogel, through the amino and catechol groups of dopamine in an organic-inorganic interface to build a covalent and non-covalent interaction. A strong attachment and an effective modulus transition system can be formed between the metal electrodes and human skin, so that the peeling force between the PDMA-PAAM hydrogel and the porcine skin can reach  $22 \text{ N m}^{-1}$ . In addition, the stable conductivity and long-term operating life of the PDMA-PAAM hydrogel for more than 60 days at room temperature are achieved by adding sodium chloride (NaCl) and glycerol, respectively. The PDMA-PAAM hydrogel membrane fabricated in this work is integrated onto a flexible Au electrode applied in a brain-computer interface. In comparison, the collected EEG signal intensity and waveform are consistent with that of the commercial counterparts. And obviously, the flexible electrode with PDMA-PAAM hydrogel membrane is demonstrated to enable a more stable and user-friendly interface.

**Keywords:** flexible electronics, dopamine, hydrogels, brain-computer interface, electroencephalogram

## INTRODUCTION

It is challenging to obtain robust data acquisition of electrical activities of neurons in the brain that control everything from the routine regulation of muscle movements to intelligent operations (e.g., memory) and are the main active representations of information transmission in the neural system [1,2]. Recording the electrical activities accurately has become a significant research subject in neuroscience. Implantable electrodes

are widely used in neuroscience research and clinical medicine [3–6]. Through implantable electrodes, the data acquisition of electroencephalogram (EEG) can be used to decode gesture information and precisely control some body actions including finger movements [7–9]. However, restricted by the dual challenges of biological compatibility [10,11] and surgical trauma [12–14], it is difficult to obtain patient-friendly implantable electrodes for long-term signal monitoring.

Benefiting from advanced flexible techniques, biological medical devices nowadays are tending to be miniaturized, lightweight and wearable. Extracorporeal patch-type medical monitoring devices and electronic devices are booming to monitor physiological signals such as electrocardiogram (ECG), electrooculogram (EOG), electromyogram (EMG) and EEG in real time [15–17]. However, induced by the modulus difference between rigid metal electrodes and soft human skin, interface mismatches lead to signal drift and performance instability of devices. Thus, to achieve an ideal interface effect including good bonding and high conductivity is of great significance to the fields of biomedical system intelligent robotics. Particularly, as the extracranial EEG signals are very weak, it is desirable to reduce the interface impedance between the electrodes and the skin to increase the interface stability and improve the comfort of wearing [18,19]. In addition, most of the electrodes are made of metal or alloy as a conductive material, resulting in a great mechanical mismatch with the skin because rigid metal materials cannot be perfectly conformal to biological tissues [20–23]. Thus, hydrogels are introduced as they are cross-linked polymers with adjustable modulus, exhibiting good compatibility, mechanical compliance and conductivity [24,25]. The high-water content of hydrogels provides a moist and ion-rich physiological environment, which can simulate the living environment of neurons. In recent years, some researchers have developed the electrodes covered with hydrogel coating to achieve the electrode-skin contact interface [26–28], and they also have used hydrogel in skin-like bioelectronic devices, such as EMG sensors [29], electronic skin [30] and high-elasticity wearable devices [31]. However, the free water in the hydrogel is prone to volatilize at room temperature, which leads to the

<sup>1</sup> Institute of Flexible Electronics Technology of THU, Zhejiang, Jiaying Key Laboratory of Flexible Electronics based Intelligent Sensing and Advanced Manufacturing Technology, Jiaying 314000, China

<sup>2</sup> AML, Department of Engineering Mechanics, Centre for Flexible Electronics Technology, Tsinghua University, Beijing 100084, China

<sup>3</sup> Qiantang Science and Technology Innovation Center, Hangzhou 310016, China

<sup>4</sup> College of Aerospace Engineering, Chongqing University, Chongqing 400044, China

\* Corresponding authors (emails: [chenying@ifet-tsinghua.org](mailto:chenying@ifet-tsinghua.org) (Chen Y); [fengxue@tsinghua.edu.cn](mailto:fengxue@tsinghua.edu.cn) (Feng X))

increasing interface impedance, signal drift and performance instability in long-term wearing [32]. Long-term stability of hydrogel-electrode interface requires hydrogels with excellent adhesive and water retention properties. A variety of studies have been carried out to add glycerol to hydrogels to improve the water retention [33–35] and adding dopamine (DA) to hydrogels to improve adhesion [36–38]. But there are still few studies on improving both water retention and adhesion, and longer water retention time is desired to achieve long-term EEG monitoring which cannot be realized in the available studies [39–42]. How to improve the quality of EEG signal collection and achieve prolonged wearing is the technical bottleneck that hinders the further development of extracranial brain electrodes.

In order to solve this problem, the polydopamine methacrylamide-polyacrylamide (PDMA-PAAM) hydrogel is designed and fabricated in our study to obtain a soft hydrogel-skin interface. The adhesive strength between the skin and electrode is effectively upgraded by the DA introduced into the hydrogel. A covalent and non-covalent interaction is built through amino and catechol groups of DA in organic-inorganic interface, so that the strong peeling force between the PDMA-PAAM hydrogel and the porcine skin can reach  $22 \text{ N m}^{-1}$ . In addition, the PDMA-PAAM hydrogel can be conductive by adding sodium chloride. Glycerol is added as a water retaining agent to improve the long-term interface stability, so that the PDMA-PAAM hydrogel can be adhesive for more than 60 days at room temperature. Applied in a brain-computer interface, the flexible electrode with PDMA-PAAM hydrogel membrane is demonstrated to enable similar function as that of commercial counterparts with a more stable interface.

## EXPERIMENTAL SECTION

### Materials

DA hydrochloride (DA-HCl, 98%), sodium tetraborate ( $\text{Na}_2\text{B}_4\text{O}_7$ , 99.5%), sodium bicarbonate ( $\text{NaHCO}_3$ , 99.8%), methacrylic anhydride (94%), tetrahydrofuran (THF, 99%), ethyl acetate (99%), *n*-hexane (97%), magnesium sulfate anhydrous ( $\text{MgSO}_4$ , AR), sodium chloride (NaCl, 99.5%) and sodium hydroxide (NaOH, 98%) were obtained from Macklin Inc. Acrylamide (AAM, 99%), ammonium persulphate (APS, 98.5%), *N,N*-methylenebisacrylamide (MBAA, AR), glycerol (99%) and tetramethylethylenediamine (TMEDA, 99.5%) were purchased from Alfa Aesar. All the materials were used as received without any further purification. Mili-Q purified water ( $18.2 \text{ M}\Omega$ ) was used for all synthesis experiments.

### Synthesis of dopamine methacrylamide (DMA)

The synthesis procedure for DMA is as follows. Sodium tetraborate (5 g) and  $\text{NaHCO}_3$  (2 g) were dissolved in 100 mL of deionized water and the oxygen in the system is removed by  $\text{N}_2$  bubbling for 30 min. DA-HCl (2.5 g, 13.2 mmol) was then added, followed by dropwise addition of methacrylic anhydride (2.35 mL, 14.5 mmol) in 25 mL of THF, during which the pH of solution was kept at about 9. The reaction mixture was stirred at room temperature with  $\text{N}_2$  bubbling for 24 h. After the reaction, the aqueous mixture was washed twice with 150 mL of ethyl acetate and then the pH of the aqueous solution was reduced to less than 2 by adding HCl aqueous and extracted three times with 100 mL of ethyl acetate. Finally, anhydrous  $\text{MgSO}_4$  was added to the ethyl acetate layer for drying. After anhydrous

$\text{MgSO}_4$  was extracted and filtered out, the volume of the mixture was reduced to about 20 mL by rotary evaporation. Then 250 mL of *n*-hexane was added with vigorous stirring and the suspension was held at 4–6°C for 12 h. The resulting mixture was pumped and dried to obtain a grey solid product (2.12 g). Fourier transform infrared (FT-IR) spectroscopy (KBr,  $\text{cm}^{-1}$ ): 3270 (N–H stretching), 1650 ( $\text{C}=\text{CH}_2$  stretching), 1582 (C=O stretching), 1549 (N–H bending), and 1526 (C–N stretching). Proton nuclear magnetic resonance ( $^1\text{H}$  NMR) (400 MHz, dimethyl sulfoxide (DMSO)):  $\delta = 7.92$  (t,  $J = 5.2$  Hz, 1H, NH), 6.60 (dd,  $J = 21.1, 4.8$  Hz, 2H), 6.43 (dd,  $J = 7.9, 1.6$  Hz, 1H), 5.61 (s, 1H,  $\text{C}=\text{CH}_2$ ), 5.30 (s, 1H,  $\text{C}=\text{CH}_2$ ), 3.22 (dd,  $J = 14.5, 6.3$  Hz, 2H,  $-\text{CH}_2-\text{CH}_2-$ ), 2.56 (dd,  $J = 15.0, 7.1$  Hz, 2H,  $-\text{CH}_2-\text{CH}_2-$ ), 1.84 (s, 3H,  $-\text{CH}_3$ ).

### Preparation of hydrogels

Taking 0.4 wt% DMA content as an example, the preparation process of the hydrogel is as follows: DMA powder (0.004 g) was added into NaOH solution (pH 11, 10 g) and magnetically stirred at  $400 \text{ r min}^{-1}$  for 3 h at room temperature to achieve the oxidation of DMA. Then, AAM (2.5 g), APS (0.1 g), MBAA (0.003 g) and TMEDA (20  $\mu\text{L}$ ) were added to the DMA solution at room temperature under stirring. After 5 min stirring, the stirrer was removed and the DMA and AAM were polymerized to form PDMA-PAAM hydrogel. FT-IR ( $\text{cm}^{-1}$ ): 3335, 1602 (N–H stretching), 2932 (C–H asym stretching), 1649 (C=O stretching), 1418 (N–H bending), and 1119 ( $\text{NH}_2$  rocking).

To prepare hydrogels with glycerol and NaCl, the obtained hydrogels were first dried at 40°C, and then soaked in glycerol and NaCl aqueous solution. In order to investigate the effect of glycerol on the water loss rate of hydrogels, the rectangular shaped dried hydrogels (40 mm  $\times$  40 mm  $\times$  1 mm) were soaked in glycerol aqueous solution with different glycerol contents (0, 10, 20, 30, 40, and 50 wt%) until completely swollen. And then they were removed from the solution, drained with qualitative filter paper on the surface to squeeze out the solvent, and placed in an oven (20°C, 40% relative humidity). The weight of the sample was recorded at regular intervals, and the weight loss was calculated from the ratio of the measured weight at time  $t$  ( $W_t$ ) to the initial weight ( $W_0$ ). Three parallel experiments were conducted for each experimental condition, and the average data were used.

In the conductivity experiments, the contents of glycerol were designed to be 20 wt%. The rectangular shaped dried hydrogels (40 mm  $\times$  40 mm  $\times$  1 mm) were soaked in glycerol and NaCl aqueous solution with different NaCl contents (0.05, 0.10, 0.15, 0.20, and 0.24 g  $\text{mL}^{-1}$ ) until completely swollen. And then they were removed from the solution, drained with qualitative filter paper on the surface to squeeze out the solvent, and placed in an oven (20°C, 40% relative humidity). The resistance signal of the sample was recorded at regular intervals. For each experimental condition, three parallel experiments were conducted and the average data were used.

### Cytotoxicity test for hydrogels

To obtain the cytotoxicity of the PDMA-PAAM hydrogels, a square PDMA-PAAM hydrogel (0.5 mm  $\times$  0.5 mm  $\times$  500  $\mu\text{m}$ ) and a PAAM hydrogel (0.5 mm  $\times$  0.5 mm  $\times$  500  $\mu\text{m}$ ) were immersed separately into human HacaT cell culture solutions for 24 h. The cells were then dyed using a Calcein-AM/PI double stain kit (Calcein-AM from Aladdin, propidium iodide (PI)

from Solarbio). Fluorescent images of dyed viable and dead cells were captured using a fluorescence microscope (Olympus IX51, Olympus Corporation).

The cell viability was evaluated by the CCK8 assay simultaneously. HacaT cells seeded in a 96-well plate were cultivated in 100  $\mu\text{L}$  of dulbecco's modified Eagle medium (DMEM) containing 10% foetal bovine serum (FBS) for one night at 37°C under a humidified 5%  $\text{CO}_2$  atm. Subsequently, 20  $\mu\text{L}$  of PAAM hydrogel or PDMA-PAAM hydrogel dispersed in 100  $\mu\text{L}$  of DMEM was added to each well, and the cells were incubated for another 24 h in the dark. Then, the medium was replaced with 110  $\mu\text{L}$  of the fresh CCK8 (CCK:DMEM = 1:10). After 0.5 h of incubation, the optical density (OD) was measured at 450 nm with a microplate reader model. The average value of the experiments was collected, and the cell viability can be obtained as follows:

$$\text{Cell viability (\%)} = (\text{OD}_{\text{sample}}/\text{OD}_{\text{blank}}) \times 100,$$

where  $\text{OD}_{\text{blank}}$  was obtained in the absence of PAAM hydrogel or PDMA-PAAM hydrogel, and  $\text{OD}_{\text{sample}}$  was obtained in the presence of PAAM hydrogel or PDMA-PAAM hydrogel.

### Instruments and measurements

A Perkin Elmer RX1 spectrometer produced by Thermo Corporation was adopted to record attenuated total reflection FT-IR spectroscopy (ATR FT-IR) at frequencies from 500 to 4000  $\text{cm}^{-1}$ .  $^1\text{H}$  NMR ( $^1\text{H}$ , 400 MHz) spectra were obtained on a Bruker AV400 spectrometer using  $\text{DMSO-d}_6$  as the solvent.

Tensile and compression tests were conducted to investigate the mechanical properties of the hydrogels by using an *in-situ* biaxial fatigue testing system (IPBF-300L, China) at room temperature. The hydrogel samples were molded into dumbbell shapes (gauge length of 20 mm, width of 5 mm, and thickness of 1 mm).

The adhesive properties of the hydrogels were tested by a 90° peeling experiment on a strength analyzer (KEXING HAK-3516B, China) with a speed of 8  $\text{mm min}^{-1}$ . The hydrogel samples were molded into rectangular shapes (length of 150 mm, width of 20 mm, and thickness of 1 mm). The deformation of the hydrogel along the peeling direction was limited due to a rigid polyethylene terephthalate (PET) film bonded to the back of the hydrogel. The hydrogel was tested by the peeling experiment at porcine skin after being pressed by an object with 200 g for 10 min at room temperature. For the tests at Au electrode, the hydrogels were pressed to a copper plate with Au deposition, due to the exfoliation of Au on PDMS. For each hydrogel sample, 3–5 specimens were tested and the average data was used.

The resistance signals were collected by a digital multimeter (Keysight 34461 A, USA). The EEG signals were recorded and analyzed by a Blackrock's Cerebus electrophysiological signal collection system. Flexible Au electrodes here were fabricated by a micro electromechanical system (MEMS) process with PDMS as the substrate. The Au electrode was attached to the human auricle with the PDMA-PAAM hydrogel membrane to a robust interface between the electrode and skin. The subjects were ordinary and healthy male adults. During the test, the EEG signals were collected from the subjects after 5 min of relaxation time during which their eyes were closed, and the collection time was 5 min. The sampling rate of all experiments was set to 1000 Hz, and an analog filter was applied with a frequency band of 0.5–200 Hz.

## RESULTS AND DISCUSSION

### Design and synthesis of DMA and PDMA-PAAM hydrogel

To prepare tough, adhesive and conductive hydrogels, DMA, glycerol and NaCl were successfully introduced into the PAAM hydrogel system as functional components. The reaction processes of DMA and PDMA-PAAM are illustrated in Fig. 1a, b, respectively. FT-IR was used to corroborate the successful graft of double bond on DA (Fig. 1c), where some notable peaks appear in the spectrum of DMA in contrast to that of DA including a peak at 1650  $\text{cm}^{-1}$  from stretching vibrations of  $\text{C}=\text{CH}_2$  group, a peak at 1582  $\text{cm}^{-1}$  from stretching vibrations of  $\text{C}=\text{O}$  group, a peak at 1549  $\text{cm}^{-1}$  from bending vibrations of  $\text{N}-\text{H}$  in the amide group, and a peak at 1526  $\text{cm}^{-1}$  from stretching vibrations of the  $\text{C}-\text{N}$  group. And the copolymerization of DMA and AAM was proved by the FT-IR spectra in Fig. 1d, where the spectrum of PDMA-PAAM changes with some notable peaks disappearing in contrast to that of AAM including a peak at 1673  $\text{cm}^{-1}$  from stretching vibrations of  $\text{C}=\text{CH}_2$  group, and peaks at 1000–675  $\text{cm}^{-1}$  from out-of-plane bending vibrations of  $\text{C}=\text{CH}_2$  group.

Under alkaline conditions, DA is first oxidized to DA-quinone followed by intramolecular cyclization *via* 1,4-Michael-type addition to yield leucodopaminechrome [43–45]. For DMA, intramolecular cyclization is prevented because the amino group is linked to the double bond. Therefore, DMA is oxidized to DA-quinone under alkaline conditions. Due to the trace content of DMA in the hydrogel, the characteristic peak of DA-quinone cannot be found in the FT-IR spectrum.

A two-step method was applied to prepare the PDMA-PAAM hydrogel as illustrated in Fig. 2. Initially, AAM monomer, MBAA (chemical cross-linker), TMEDA (curing catalyst) and APS (initiator) are completely dissolved in oxidized DMA solution, and the PDMA-PAAM hydrogel is formed *in situ* *via* the radical polymerization of DMA and AAM monomers. Subsequently, the obtained hydrogels are dried in 40°C, and then soaked in glycerol and NaCl aqueous solution to make glycerol replace part of water, which improves the long-term stability of the hydrogel through the hydrogen bonds between water and glycerol. Furthermore, the addition of NaCl provides ions for the hydrogel, endowing the PDMA-PAAM hydrogel with ionic conductivity.

### Mechanical properties

To investigate the mechanical properties of the PDMA-PAAM hydrogel, a series of tensile and compression experiments were conducted. Fig. 3a shows the stress-strain curves for the PDMA-PAAM hydrogel with different DMA contents, which indicates that the mechanical properties of the PDMA-PAAM hydrogel are significantly influenced and can be tailored by controlling the content of DMA. With the increase of DMA content, the propagation at break decreases, indicating that the addition of DMA has an adverse effect on the generation of PAAM cross-linking network. The catechol group in DA can capture free radicals of the system during AAM polymerization, which hinders the propagation of polymer molecular chain [46,47]. Therefore, an effective polymer network cannot be formed, resulting in poor mechanical properties of the PDMA-PAAM hydrogel.

To further confirm the effect of DMA on polymerization, the gelation experiments with DMA contents of 0.4, 0.45, 0.5, 0.6,

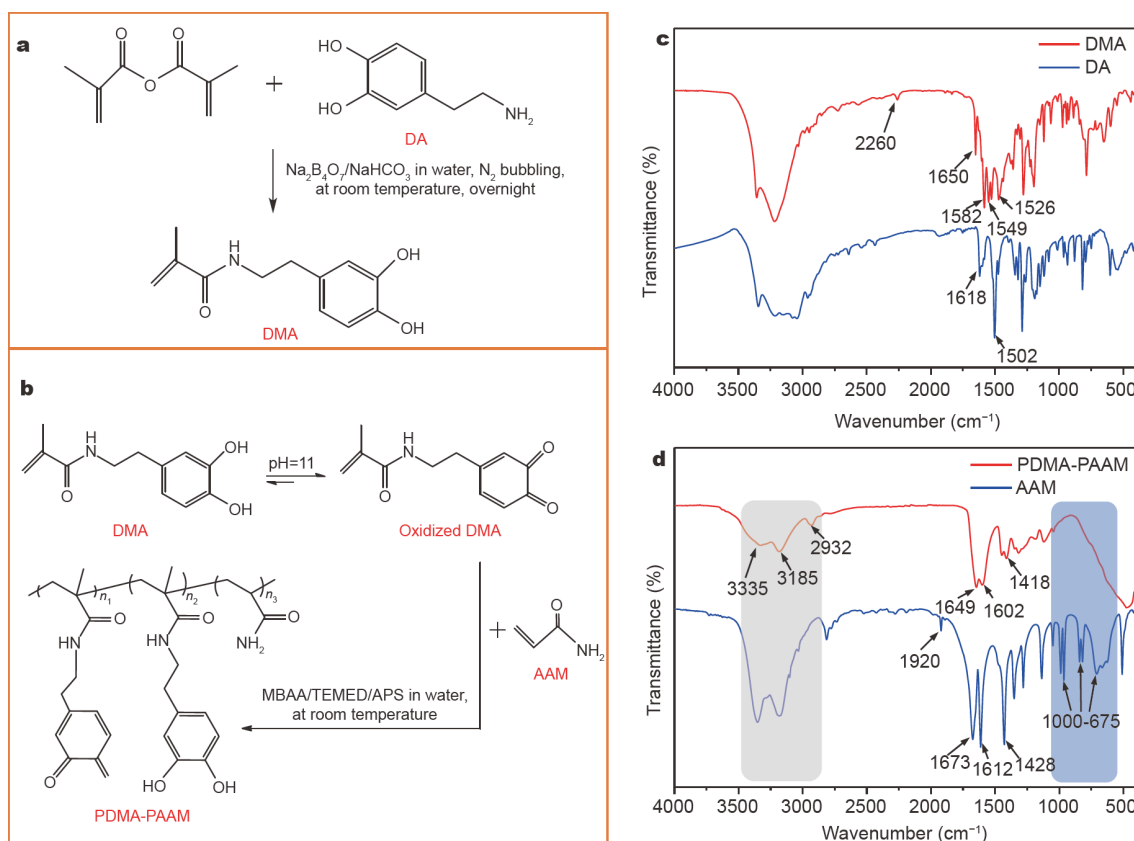


**Figure 1** Reaction process for the synthesis of (a) DMA and (b) PDMA-PAAM along with their chemical structures; FT-IR spectra of (c) DA, DMA and (d) AAM, PDMA-PAAM.

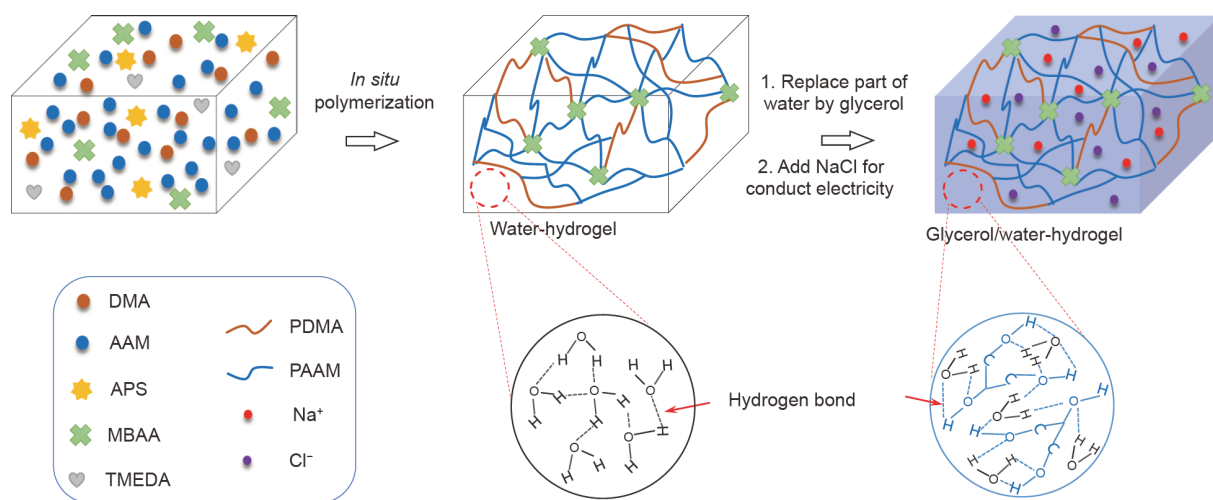


**Figure 2** Schematic diagram of the hydrogel synthetic progress including the *in-situ* polymerization to form the PDMA-PAAM hydrogel and immersion of the hydrogel in glycerol and NaCl aqueous solution to improve long-term stability and conductivity.

0.8, and 1.0 wt% were performed. The results are shown in Fig. S1. When the content of DMA is 0.4 wt%, AAM can polymerize effectively to form gel. When the content of DMA is 0.45 and 0.50 wt%, viscous fluids are formed in the system. When the content of DMA is greater than 0.50 wt%, AAM monomers will not be polymerized and the system remains to be liquid with low viscosity. The gelation experiments showed that DMA hinders the propagation of polymer molecular chain, and further reduces

the mechanical properties of hydrogels. However, when the DMA content is 0.4 wt%, the failure of the PDMA-PAAM hydrogel occurs at the elongation of 600%, indicating that the PDMA-PAAM hydrogel with 0.4 wt% DMA exhibits good mechanical properties.

Tensile tests in Fig. 3b show that the stress-strain curves coincide basically when the PDMA-PAAM hydrogel with DMA content of 0.3 wt% is stretched to 1000% at different strain rates,

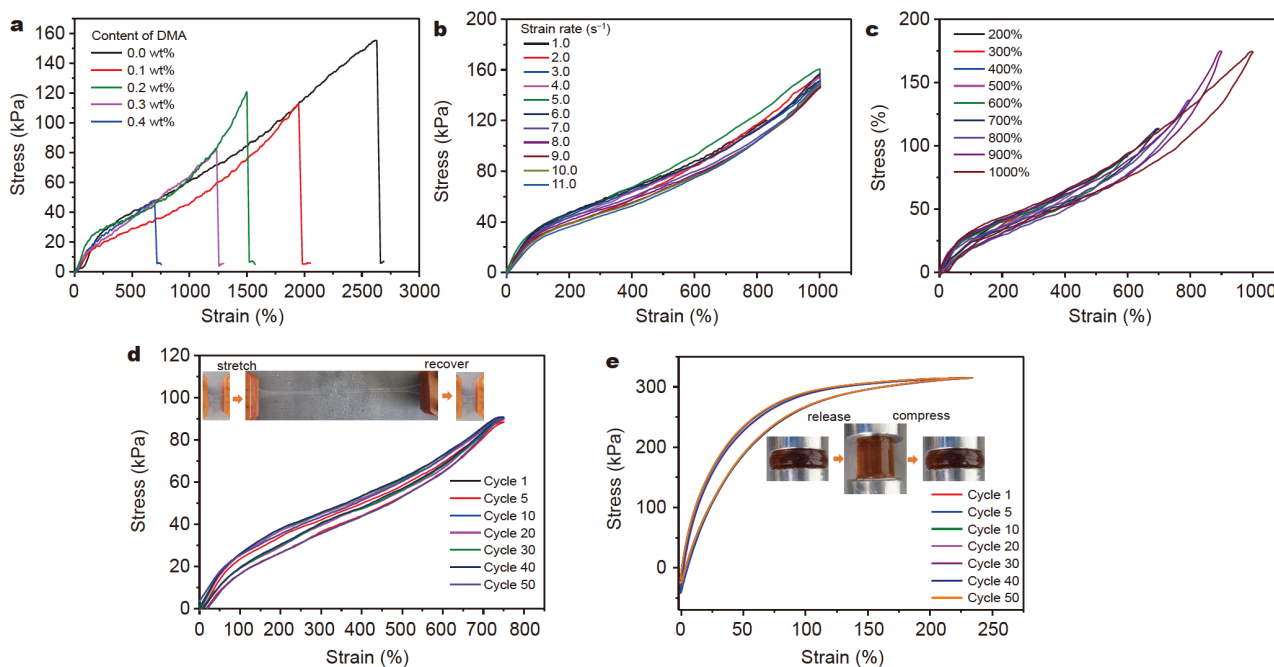


**Figure 3** Mechanical properties of the PDMA-PAAM hydrogel. (a) Stress-strain curves for the PDMA-PAAM hydrogel with different DMA contents. (b) Tensile properties for PDMA-PAAM-0.3 at different strain rates. (c) Cyclic tensile loading-unloading curves under different strains. (d) Continuous cyclic tensile loading-unloading curves at 750% strain without resting time after each cycle (the inset image shows the stretch-recover process). (e) Typical successive loading-unloading compression tests of the PDMA-PAAM hydrogel at 230% strain without resting intervals (the inset image shows the compress-release process).

indicating that the strain rate of the PDMA-PAAM hydrogel has no inertia. In the hydrogel system, the polymer molecular chain is in a water-rich environment, and the water molecules absorb part of the energy during loading. In the rapid loading, the molecular chain still has enough space and timely structural rearrangement. Therefore, the mechanical response curves of hydrogels are very close under fast and slow loading conditions.

The energy hysteresis behavior and the self-recovery ability of the PDMA-PAAM hydrogel were studied by the successive cyclic loading-unloading tests at different strains. As shown in Fig. 3c, the dissipated energy of the hydrogel significantly increases with the strain from 200% to 1000%. As the strain increases, more cross-linked bonds are destroyed, dissipating a large amount of energy and leading to the extension of recovery time.

The cyclic hysteresis loop can characterize the failure characteristics of materials. According to the hysteresis loop in Fig. 3d, the tensile loading curve and the unloading curve basically coincide, indicating that no damage occurs in the process of stretching and the PDMA-PAAM hydrogel maintains good elastic recovery ability. In addition, after 50 cycles, the loading-unloading curve of the PDMA-PAAM hydrogel still maintains a good coincidence, indicating that within this strain range, the PDMA-PAAM hydrogel has a good anti-cyclic loading ability. In the compression state, the unloading curve lags behind the loading curve, but it can still recover to the initial state in this period of time as shown in Fig. 3e. Within 50 cycles, the convergence degree of hysteresis loop of the PDMA-PAAM hydrogel is high, indicating that the material can be restored to the initial state in time within this loading frequency, and the PDMA-PAAM hydrogel has good compression resilience.

The above mechanical tests show that the PDMA-PAAM

hydrogel has good mechanical properties. In addition, the mechanical properties of PAAM hydrogel are applied as a control (Fig. S2), which has similar stress-strain curves and cyclic hysteresis loop, indicating that the addition of DMA has little effect on the mechanical properties of hydrogels in the range of gelation. To collect physiological signals, flexible electrodes need to deform as the skin deforms. The mechanical stability of the interface material is beneficial for keeping the stability of the electrode in the process of repeated peeling and pasting. Therefore, the PDMA-PAAM hydrogel is an excellent interface material for physiological signal electrodes.

#### Adhesive properties

The adhesion property of the hydrogel is a very important index, which directly determines the interface stability. Porcine skin is selected for the *in vitro* experiments due to its very similar characteristic to human skin. The PDMA-PAAM hydrogel exhibits excellent adhesiveness to the porcine skin due to the catechol groups in DA, which can mimic the adhesion mechanism of mussel. As shown in Fig. 4a, there are a lot of catechol groups from DMA, which can form chemical interactions with sulfhydryl and amino groups on the surface of biological tissues [48–50]. Furthermore, the amide groups on the surface of biological tissues can form hydrogen bonds with amido groups from AAM and hydroxy groups from DMA.

To evaluate the adhesive properties of the PDMA-PAAM hydrogel, a 90° peeling test was performed to measure the peeling force between the hydrogel and the porcine skin, and the results are shown in Fig. 4b. It is found that the content of DMA significantly influences the adhesive strength. With the increase of DMA content, the adhesive peeling force of the PDMA-PAAM hydrogel increases, but the increasing trend slows down.

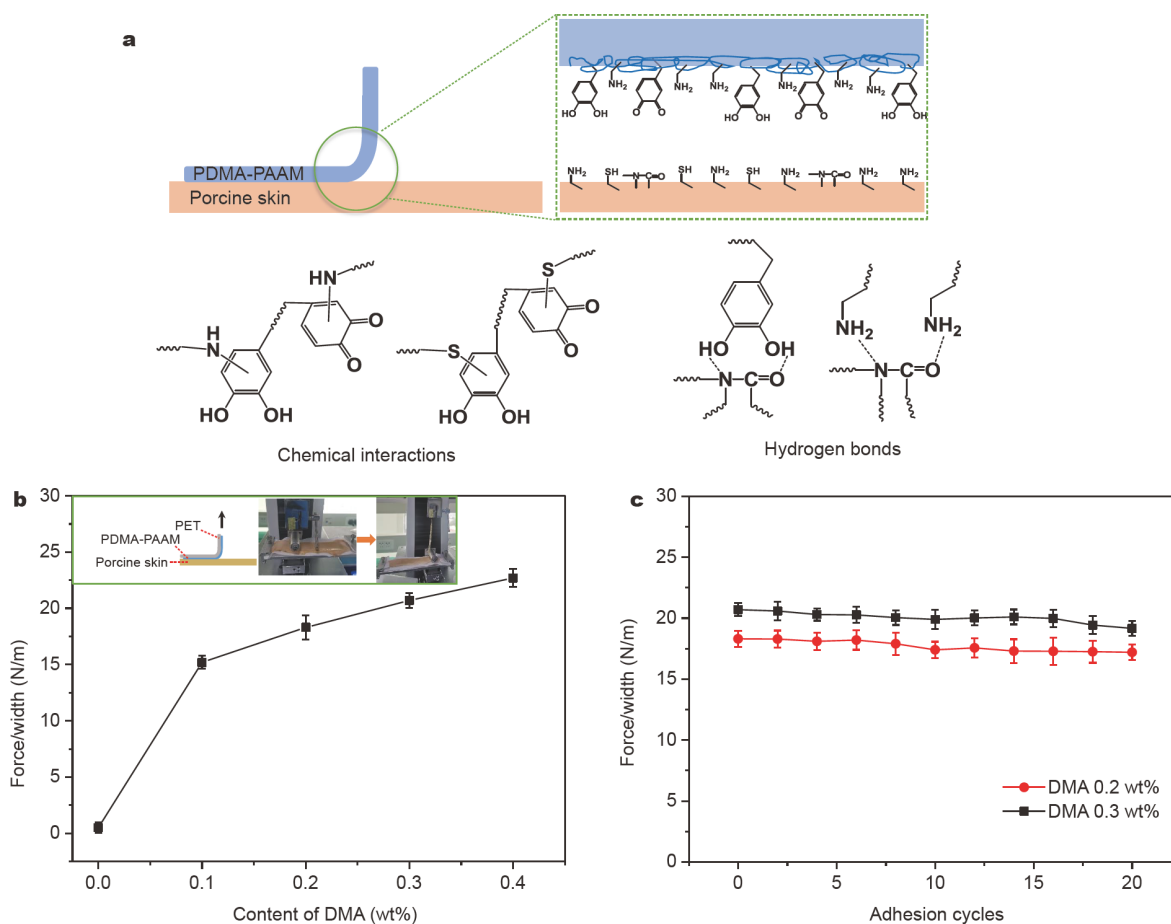


**Figure 4** (a) Schematic depiction of the adhesion mechanism. (b) Peeling curves of the PDMA-PAAM hydrogel on porcine skin (the inset images show the peeling process). (c) Twenty-time cyclic peeling tests of the PDMA-PAAM hydrogel on the porcine skin.

As the previous experimental results show that the increase of DMA content reduces the elongation at break of the hydrogel, by considering the mechanical and adhesion properties simultaneously, the cyclic peeling tests were performed on the PDMA-PAAM hydrogel with DMA contents of 0.2 and 0.3 wt%, respectively. As shown in Fig. 4c, twenty-time cyclic peeling tests of the PDMA-PAAM hydrogel were performed on the porcine skin. The adhesive strength almost remains after 20 times of peeling process, indicating that the PDMA-PAAM hydrogel has stable adhesion property.

In addition, the adhesive experiment of PDMA-PAAM to Au electrode was performed on a copper plate with Au deposition, due to the exfoliation of Au on PDMS. As shown in Fig. S3a, the peeling force is  $60 \text{ N m}^{-1}$  when the content of DMA is 0.4 wt%, suggesting good adhesion of the PDMA-PAAM hydrogel to the Au electrode. And the adhesive strength is stable with twenty-time cyclic peeling tests, as shown in Fig. S3b.

#### Long-term stability and conductivity

The long-term stability of the PDMA-PAAM hydrogel is demonstrated by its weight at different time intervals as shown in Fig. 5a. At the beginning of exposure, each sample loses weight rapidly. However, the weight loss of the PDMA-PAAM hydrogel decreases obviously after the addition of glycerol. The hydrogel remains moist after a prolonged storage in normal conditions for 60 days, attributed to the effective water retention

through glycerol-water interactions. When the content of glycerol is greater than 20 wt%, the final PDMA-PAAM hydrogel holds more water. In comparison, the PDMA-PAAM hydrogel without glycerol quickly loses its weight, close to its original water content after 2 days, and finally becomes a dried copolymer.

However, the addition of glycerol decreases the adhesive strength of the PDMA-PAAM hydrogel. It may be due to that the water absorption of glycerol leads to the formation of a water film at the interface, which hinders the formation of chemical bonds and hydrogen bonds, failing to form effective adhesion. According to the previous description, under the consideration of the mechanical properties and adhesion properties, different glycerol content experiments were carried out for the hydrogels with the DMA content of 0.3 wt%. As shown in Fig. 5b, with the increase of glycerol content, the peeling force decreases slightly, but when the glycerol content is 50 wt%, the peeling force can still reach  $12.9 \text{ N m}^{-1}$ , indicating the remarkable adhesive property. And the adhesive curve of PDMA-PAAM on the Au electrode has the similar trend, as shown in Fig. S3c.

The PDMA-PAAM hydrogel possesses high conductivity due to the addition of NaCl which provides ions in the hydrogel. As shown in Fig. 5c, the resistance of the PDMA-PAAM hydrogel decreases with increasing NaCl concentration. When the concentration exceeds  $0.1 \text{ g mL}^{-1}$ , the resistance remains stable at about  $20 \text{ k}\Omega \text{ cm}$ , indicating the saturation of ions in the

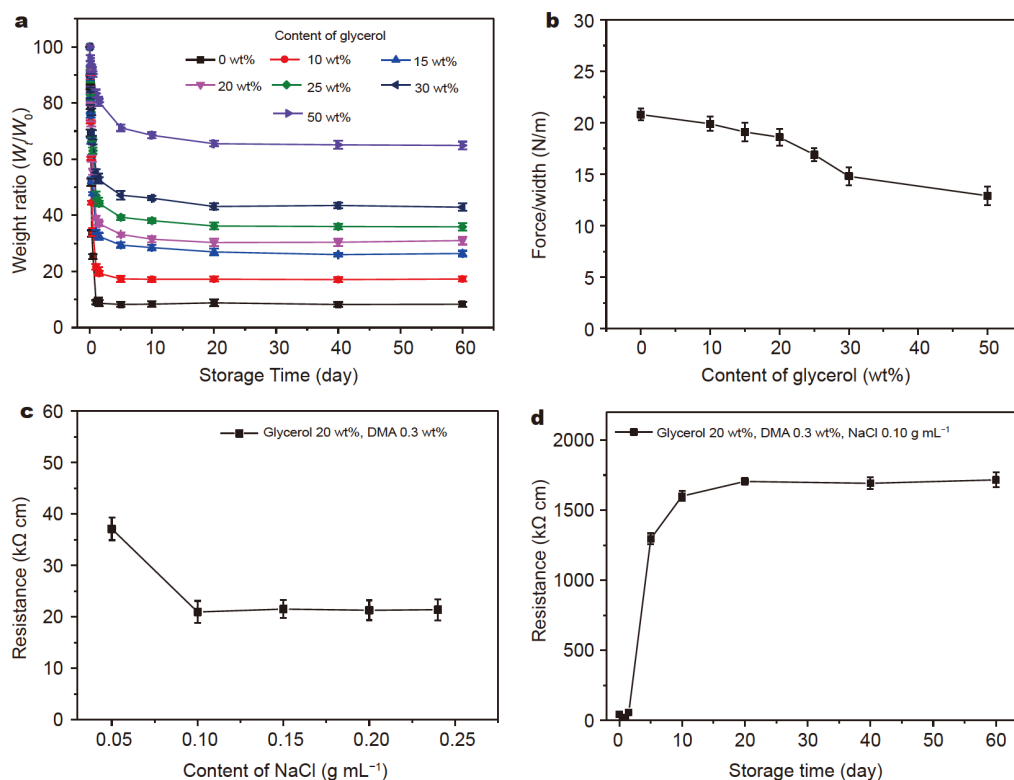


**Figure 5** (a) Weight change of the PDMA-PAAM hydrogel with different glycerol contents as a function of storage time. (b) Peeling curves of the PDMA-PAAM hydrogel with different glycerol contents on porcine skin. (c) The effect of NaCl content on the resistance of the PDMA-PAAM. (d) The resistance of the PDMA-PAAM hydrogel as a function of the storage time with the contents of NaCl of 0.10 g mL<sup>-1</sup>.

hydrogel. With the increase of storage time, the resistance increases gradually and tends to be stable, as shown in Fig. 5d. In the early stage, the water volatilization slows the flow of ions in the hydrogel, so the resistance increases. With the stability of water content in the system, the resistance also tends to be stable.

The effects of the above functional components on the performance of the PDMA-PAAM hydrogel are summarized as follows: (1) adding DMA into the system can improve the adhesive property, but a too high DMA content will reduce the mechanical properties of the hydrogel. (2) Glycerol can improve the long-term storage stability, but too much glycerol will lead to the decline of adhesive property. (3) NaCl is added to improve the conductivity, but too much NaCl will form a saturated solution, resulting in no more change of conductivity. Taking adhesion, long-term stability and conductivity properties into consideration, DMA content of 0.3 wt%, glycerol content of 20 wt% and NaCl content of 0.10 g mL<sup>-1</sup> is finally tailored to be the optimal scheme for the application experiments.

In addition, the elastic moduli of the hydrogels with various compositions were calculated through the stress-strain curves, and the results are shown in Table S1. The elastic modulus of the hydrogels decreases with increasing DMA contents, suggesting the decrease of the polymer network density. It is consistent with the effect of DMA on the mechanical properties of PDMA-PAAM hydrogels mentioned above. And with the increase of glycerol and NaCl contents, the elastic modulus of hydrogels increases slightly, indicating the increase of intermolecular hydrogen bonds in the hydrogels. The elastic moduli of hydrogels with various compositions are all at kPa level, which can

match the elastic modulus of human skin (MPa), avoiding the signal drift caused by modulus mismatch.

#### Cytotoxicity tests

Verified by cytotoxicity evaluation, the PDMA-PAAM hydrogels may have promising application in the direct contact interface between human skin and devices. The PDMA-PAAM hydrogel and a reference PAAM hydrogel were both immersed into two human HacaT cell culture solutions for 24 h. The fluorescent images in Fig. 6a show the living (green) and dead (red) cells are dyed by a Calcein-AM/PI double stain assay. The images show that there are more than 98% of living cells with and without the presence of PDMA-PAAM hydrogels, suggesting the PDMA-PAAM hydrogels are biologically safe. The cytotoxicity test was also conducted using a CCK8 assay. The viability of cells within the culture solution immersed with the PDMA-PAAM hydrogels is 98.40%, as shown in Fig. 6b, satisfying the required 70% cell viability as recommended by United States Pharmacopoeia (USP) (ISO 10993-5) [47,50,51]. The cytotoxicity tests suggest that the PDMA-PAAM hydrogels are biocompatible to cells for long-term skin contact study.

#### Application in brain-computer interface

Compared with EMG and EOG, EEG signals are weak and difficult to be monitored. In order to verify the actual effect of the PDMA-PAAM hydrogel in physiological signal acquisition, it is applied to a flexible wearable EEG acquisition system. Alpha waves are the EEG signals from 8 to 13 Hz, representing the brain activities when the subject is in a wakeful relaxed state with closed eyes, and the waves are reduced when the subject opens

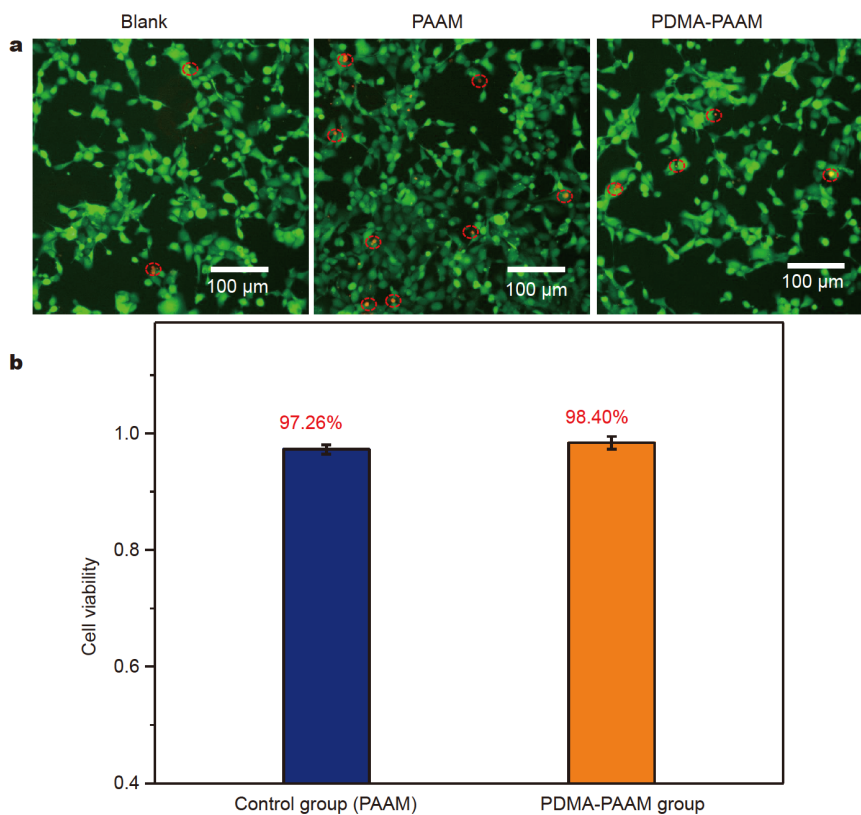


**Figure 6** Cytotoxicity test and demonstration of the applications of hydrogels. (a) Fluorescent images of the dyed viable (green) and dead (red) cells using the Calcein-AM/PI double stain assay for a blank solution without any hydrogels and solutions with PAAM hydrogels or PDMA-PAAM hydrogels after 24 h incubation. (b) Cell viability obtained using the CCK8 assay after 24 h hydrogels incubation.

eyes, is drowsy or sleeping [52]. Theta waves are the EEG signals with a frequency between 4 and 8 Hz, and are usually found in meditative, drowsy, hypnotic, or sleep states. Detecting the alpha and theta waves in the EEG is very useful for obtaining the mental state of the user in the brain-computer interface system. In this study, EEG signals of alpha and theta waves were collected respectively through traditional electrodes and the flexible electrode with PDMA-PAAM membrane. And the comparison was carried out here.

Fig. 7a shows the schematic diagram of the flexible electrode with PDMA-PAAM membrane attached to the human auricle for testing. Fig. 7b shows two periods of EEG signals, of which alpha and theta waves are measured when the subjects are approaching their eyes, corresponding to the flexible electrode with PDMA-PAAM membrane and the traditional electrode applied at the left and right auricles of the human body respectively. The spectra of EEG signals measured by both electrodes show a similar change tendency. The EEG signals is amplified at 2.5–5.5 s to obtain the EEG signals as shown in Fig. 7c, from which it can be seen clearly that the alpha and theta waves of EEG measured by the two electrodes are basically the same, indicating that the flexible electrode with PDMA-PAAM membrane can be successfully used for the recording of EEG signals. As shown in Fig. 7d, frequency-domain signals are measured under the eye-closed state when the flexible electrode with PDMA-PAAM membrane is applied at the left auricle of human body and the traditional electrode is applied at the left auricle of the human body. Our electrodes show prominent theta and alpha wave peaks around 4–8 and 8–13 Hz respectively, as

expected for normal EEG activity when the subjects' eyes are closed. The time-frequency diagram in Fig. 7e further demonstrates this conclusion. In the test time of 50 s, the highest intensity signals are about 5 and 12 Hz, indicating that the signals are theta and alpha waves of EEG signals.

To demonstrate long-term stable interface for EEG recording, EEG signals were measured by the Au electrode with PDMA-PAAM membrane exposed at room temperature for 30 and 60 days, as shown in Fig. S4. The result suggests that the alpha waves of EEG could still be detected clearly, indicating that the PDMA-PAAM hydrogel could be used to measure the EEG signals stably for a long time.

## CONCLUSIONS

In summary, a soft and effective hydrogel-skin interface is achieved by the PDMA-PAAM hydrogel designed and fabricated in this work. The introduced DMA increases the adhesive strength through amino and catechol groups of DMA in organic-inorganic interface to build a covalent and non-covalent interaction. The PDMA-PAAM hydrogel exhibits excellent cyclic strain loading resistance and compression resilience. The good elastic resilience is also demonstrated as the PDMA-PAAM hydrogel can recover to the initial state when stretched for 50 cycles at 750% strain or compressed for 50 cycles at 230% strain. In addition, glycerol is added to the hydrogels as a water retaining agent to improve the long-term stability of the interface, rendering the PDMA-PAAM hydrogel good flexibility and adhesion for more than 60 days at room temperature. NaCl is added as a conductive component to ensure the stability of

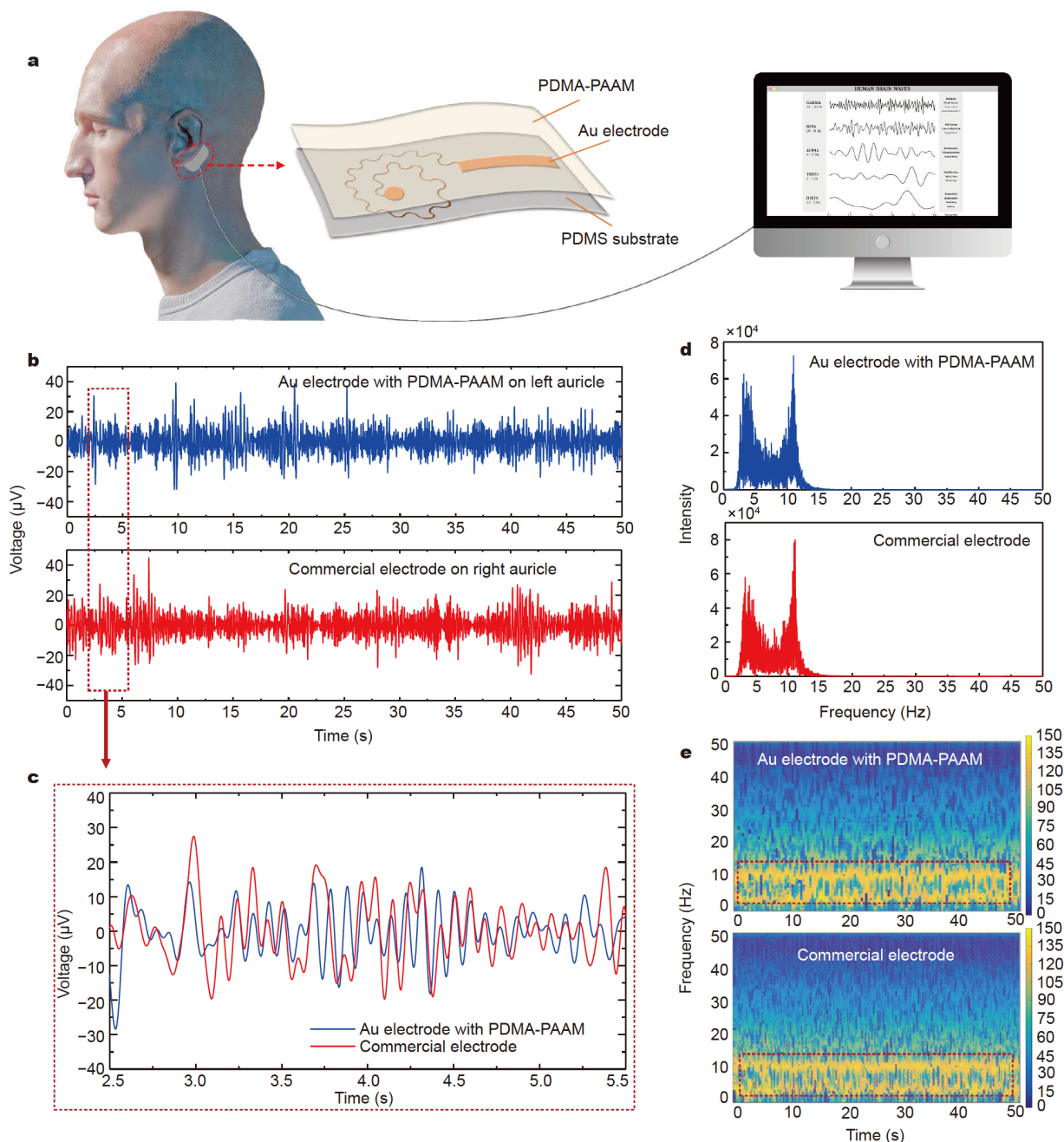


**Figure 7** (a) Schematic diagram of the flexible electrode with the PDMA-PAAM membrane attached to the human auricle for testing. (b) Time-domain spectrogram of EEG alpha band measured under eyes closed state when the flexible electrode with PDMA-PAAM membrane and the traditional electrode are applied at the left and right auricles of the human body, respectively. (c) Amplification of the time-domain signals at 2.5–5.5 s in (b). Frequency-domain spectrogram (d) and time-frequency spectrogram (e) of EEG alpha band measured under eyes closed state when the flexible electrode with PDMA-PAAM membrane is applied at the left auricle of human body and the commercial electrode at the right auricle.

interfacial impedance. The hydrogel is applied to a Au electrode as the interface material between the electrode and skin, and the EEG signals are successfully measured which are similar to that of commercial electrodes.

Received 28 March 2022; accepted 2 June 2022;  
published online 15 June 2022

- 1 Nelson PG, Brenneman DE. Electrical activity of neurons and development of the brain. *Trends Neurosci*, 1982, 5: 229–232
- 2 Alivisatos AP, Andrews AM, Boyden ES, *et al.* Nanotools for neuroscience and brain activity mapping. *ACS Nano*, 2013, 7: 1850–1866

- 3 Ma Y, Zhang Y, Cai S, *et al.* Flexible hybrid electronics for digital healthcare. *Adv Mater*, 2020, 32: 1902062
- 4 Mineev IR, Musienko P, Hirsch A, *et al.* Electronic dura mater for long-term multimodal neural interfaces. *Science*, 2015, 347: 159–163
- 5 Rios G, Lubenov EV, Chi D, *et al.* Nanofabricated neural probes for dense 3-D recordings of brain activity. *Nano Lett*, 2016, 16: 6857–6862
- 6 Wang J, Thow XY, Wang H, *et al.* A highly selective 3D spiked ultraflexible neural (SUN) interface for decoding peripheral nerve sensory information. *Adv Healthcare Mater*, 2017, 7: 1700987
- 7 Lee B, Koripalli MK, Jia Y, *et al.* An implantable peripheral nerve recording and stimulation system for experiments on freely moving animal subjects. *Sci Rep*, 2018, 8: 6115

- 8 Yang J, Liu L, Li T, *et al.* Array focal cortical stimulation enhances motor function recovery and brain remodeling in a rat model of ischemia. *J Stroke Cerebrovasc Dis*, 2017, 26: 658–665
- 9 Nam J, Lim HK, Kim NH, *et al.* Supramolecular peptide hydrogel-based soft neural interface augments brain signals through a three-dimensional electrical network. *ACS Nano*, 2020, 14: 664–675
- 10 Grill WM, Norman SE, Bellamkonda RV. Implanted neural interfaces: Biochallenges and engineered solutions. *Annu Rev Biomed Eng*, 2009, 11: 1–24
- 11 Bettinger CJ. Recent advances in materials and flexible electronics for peripheral nerve interfaces. *Bioelectron Med*, 2018, 4: 1
- 12 Won SM, Song E, Zhao J, *et al.* Recent advances in materials, devices, and systems for neural interfaces. *Adv Mater*, 2018, 30: 1800534
- 13 Lee M, Shim HJ, Choi C, *et al.* Soft high-resolution neural interfacing probes: Materials and design approaches. *Nano Lett*, 2019, 19: 2741–2749
- 14 Li H, Liu H, Sun M, *et al.* 3D interfacing between soft electronic tools and complex biological tissues. *Adv Mater*, 2021, 33: 2004425
- 15 Pedrosa P, Fiedler P, Schinaia L, *et al.* Alginate-based hydrogels as an alternative to electrolytic gels for rapid EEG monitoring and easy cleaning procedures. *Sens Actuat B-Chem*, 2017, 247: 273–283
- 16 Chen Y, Liu F, Lu B, *et al.* Skin-like hybrid integrated circuits conformal to face for continuous respiratory monitoring. *Adv Electron Mater*, 2020, 6: 2000145
- 17 Debener S, Emkes R, De Vos M, *et al.* Unobtrusive ambulatory EEG using a smartphone and flexible printed electrodes around the ear. *Sci Rep*, 2015, 5: 16743
- 18 Valentin O, Viallet G, Delnavaz A, *et al.* Custom-fitted in- and around-the-ear sensors for unobtrusive and on-the-go EEG acquisitions: Development and validation. *Sensors*, 2021, 21: 2953
- 19 Jiang X, Bian GB, Tian Z. Removal of artifacts from EEG signals: A review. *Sensors*, 2019, 19: 987
- 20 Frankel MA, Lehmkuhle MJ, Watson M, *et al.* Electrographic seizure monitoring with a novel, wireless, single-channel EEG sensor. *Clin Neurophysiol Pract*, 2021, 6: 172–178
- 21 Bleichner MG, Debener S. Concealed, unobtrusive ear-centered EEG acquisition: cEEGrids for transparent EEG. *Front Hum Neurosci*, 2017, 11: 163
- 22 Bleichner MG, Mirkovic B, Debener S. Identifying auditory attention with ear-EEG: cEEGrid *versus* high-density cap-EEG comparison. *J Neural Eng*, 2016, 13: 066004
- 23 Sterr A, Ebajemito JK, Mikkelsen KB, *et al.* Sleep EEG derived from behind-the-ear electrodes (cEEGrid) compared to standard polysomnography: A proof of concept study. *Front Hum Neurosci*, 2018, 12: 452
- 24 Sheng H, Wang X, Kong N, *et al.* Neural interfaces by hydrogels. *Extreme Mech Lett*, 2019, 30: 100510
- 25 Yuk H, Lu B, Lin S, *et al.* 3D printing of conducting polymers. *Nat Commun*, 2020, 11: 1604
- 26 Wong TH, Yiu CK, Zhou J, *et al.* Tattoo-like epidermal electronics as skin sensors for human machine interfaces. *Soft Sci*, 2021, 1: 10
- 27 Oribe S, Yoshida S, Kusama S, *et al.* Hydrogel-based organic subdural electrode with high conformability to brain surface. *Sci Rep*, 2019, 9: 13379
- 28 Wirthl D, Pichler R, Drack M, *et al.* Instant tough bonding of hydrogels for soft machines and electronics. *Sci Adv*, 2017, 3: e1700053
- 29 Kim SH, Jung S, Yoon IS, *et al.* Ultrastretchable conductor fabricated on skin-like hydrogel-elastomer hybrid substrates for skin electronics. *Adv Mater*, 2018, 30: 1800109
- 30 Zhu J, Zhou C, Zhang M. Recent progress in flexible tactile sensor systems: From design to application. *SS*, 2021, 1: 3
- 31 Lim C, Hong YJ, Jung J, *et al.* Tissue-like skin-device interface for wearable bioelectronics by using ultrasoft, mass-permeable, and low-impedance hydrogels. *Sci Adv*, 2021, 7: eabd3716
- 32 Wellman SM, Eles JR, Ludwig KA, *et al.* A materials roadmap to functional neural interface design. *Adv Funct Mater*, 2017, 28: 1701269
- 33 Ge W, Cao S, Yang Y, *et al.* Nanocellulose/LiCl systems enable conductive and stretchable electrolyte hydrogels with tolerance to dehydration and extreme cold conditions. *Chem Eng J*, 2021, 408: 127306
- 34 Pan X, Wang Q, Ning D, *et al.* Ultraflexible self-healing guar gum-glycerol hydrogel with injectable, antifreeze, and strain-sensitive properties. *ACS Biomater Sci Eng*, 2018, 4: 3397–3404
- 35 Peng S, Liu S, Sun Y, *et al.* Facile preparation and characterization of poly(vinyl alcohol)-NaCl-glycerol supramolecular hydrogel electrolyte. *Eur Polym J*, 2018, 106: 206–213
- 36 Zhang Q, Liu X, Duan L, *et al.* Ultra-stretchable wearable strain sensors based on skin-inspired adhesive, tough and conductive hydrogels. *Chem Eng J*, 2019, 365: 10–19
- 37 Shao C, Wang M, Meng L, *et al.* Mussel-inspired cellulose nanocomposite tough hydrogels with synergistic self-healing, adhesive, and strain-sensitive properties. *Chem Mater*, 2018, 30: 3110–3121
- 38 He X, Liu L, Han H, *et al.* Bioinspired and microgel-tackified adhesive hydrogel with rapid self-healing and high stretchability. *Macromolecules*, 2018, 52: 72–80
- 39 Han L, Liu K, Wang M, *et al.* Mussel-inspired adhesive and conductive hydrogel with long-lasting moisture and extreme temperature tolerance. *Adv Funct Mater*, 2017, 28: 1704195
- 40 Wu L, Li L, Qu M, *et al.* Mussel-inspired self-adhesive, antidrying, and antifreezing poly(acrylic acid)/bentonite/polydopamine hybrid glycerol-hydrogel and the sensing application. *ACS Appl Polym Mater*, 2020, 2: 3094–3106
- 41 Yan Y, Huang J, Qiu X, *et al.* An ultra-stretchable glycerol-ionic hybrid hydrogel with reversible gelid adhesion. *J Colloid Interface Sci*, 2021, 582: 187–200
- 42 Zhu HW, Zhang JN, Su P, *et al.* Strong adhesion of poly(vinyl alcohol)-glycerol hydrogels onto metal substrates for marine antifouling applications. *Soft Matter*, 2020, 16: 709–717
- 43 Dreyer DR, Miller DJ, Freeman BD, *et al.* Elucidating the structure of poly(dopamine). *Langmuir*, 2012, 28: 6428–6435
- 44 Liebscher J, Mrówczyński R, Scheidt HA, *et al.* Structure of polydopamine: A never-ending story? *Langmuir*, 2013, 29: 10539–10548
- 45 Liu Y, Ai K, Lu L. Polydopamine and its derivative materials: Synthesis and promising applications in energy, environmental, and biomedical fields. *Chem Rev*, 2014, 114: 5057–5115
- 46 Han L, Lu X, Wang M, *et al.* A mussel-inspired conductive, self-adhesive, and self-healable tough hydrogel as cell stimulators and implantable bioelectronics. *Small*, 2017, 13: 1601916
- 47 Yu QH, Zhang CM, Jiang ZW, *et al.* Mussel-inspired adhesive polydopamine-functionalized hyaluronic acid hydrogel with potential bacterial inhibition. *Glob Challenges*, 2020, 4: 1900068
- 48 Han L, Wang M, Li P, *et al.* Mussel-inspired tissue-adhesive hydrogel based on the polydopamine-chondroitin sulfate complex for growth-factor-free cartilage regeneration. *ACS Appl Mater Interfaces*, 2018, 10: 28015–28026
- 49 Yang Z, Huang R, Zheng B, *et al.* Highly stretchable, adhesive, biocompatible, and antibacterial hydrogel dressings for wound healing. *Adv Sci*, 2021, 8: 2003627
- 50 Han L, Lu X, Liu K, *et al.* Mussel-inspired adhesive and tough hydrogel based on nanoclay confined dopamine polymerization. *ACS Nano*, 2017, 11: 2561–2574
- 51 Wang C, Zhao N, Yuan W. NIR/thermoreponsive injectable self-healing hydrogels containing polydopamine nanoparticles for efficient synergistic cancer thermochemotherapy. *ACS Appl Mater Interfaces*, 2020, 12: 9118–9131
- 52 Kaveh R, Doong J, Zhou A, *et al.* Wireless user-generic ear EEG. *IEEE Trans Biomed Circuits Syst*, 2020, 14: 727–737

**Acknowledgements** This work was supported by the National Natural Science Foundation of China (U20A6001, 11921002, and 11902292), Zhejiang Province Key Research and Development Project (2021C01183, 2020C05004, and 2021C05007-4), and the Natural Science Foundation of Zhejiang Province of China (LQ19E030003).

**Author contributions** Liu L and Liu Y designed the samples, performed the experiments and analyzed the data; Liu L wrote the paper with support from Tang R, Ai J and Ma Y; Chen Y and Feng X helped to analyze the data and conceived the framework of this paper. All authors contributed to the

general discussion.

**Conflict of interest** The authors declare that they have no conflict of interest.

**Supplementary information** Supporting data are available in the online version of the paper.



**Lanlan Liu** received her PhD degree in chemistry from Beijing University of Chemical Technology in 2014, and then worked as a postdoc at the Institute of Chemistry, Chinese Academy of Sciences during 2014 to 2017. Currently, she is an associate researcher at the Institute of Flexible Electronics Technology of Tsinghua University (THU), Zhejiang. Her research focuses on flexible conductive materials, interfaces and devices, and their applications in the biomedical field.



**Ying Chen** received her PhD degree in solid mechanics from THU, Beijing in 2017. Currently, she is an associate researcher at the Institute of Flexible Electronics Technology of THU, Zhejiang and doing her postdoctoral research at Zhejiang University. She is working as the deputy director of Soft Matter Mechanics Committee of Zhejiang Society of Theoretical and Applied Mechanics. Her research interests include the mechanical design, MEMS fabrication and performance reliability analysis of flexible electronic devices.



**Xue Feng** received his PhD degree in mechanics from THU in 2003 and then worked as a postdoc at the University of Illinois at Urbana-Champaign during 2004 to 2007. From 2005 to 2006, he also worked as a postdoc at California Institute of Technology (Caltech). He joined THU in 2007. He is now a tenure professor of the School of Aerospace Engineering, THU, and he also serves as the director of the Ministry of Education Key Laboratory of Applied Mechanics of THU. His research focuses on the fundamental and applied science in flexible electronic technology, including the mechanics design and inorganic materials enabled integrated flexible devices.

## 高稳定、低电阻聚多巴胺甲基丙烯酸酰胺-聚丙烯酰胺水凝胶及其在脑机接口中的应用

刘兰兰<sup>1</sup>, 刘亚风<sup>4</sup>, 唐瑞涛<sup>1</sup>, 艾骏<sup>1</sup>, 马寅皓<sup>2</sup>, 陈颖<sup>1,3\*</sup>, 冯雪<sup>2\*</sup>

**摘要** 硬质金属电极与柔软人体皮肤之间的界面失效会导致脑机接口器件的信号漂移和性能不稳定, 影响脑电信号的精确采集. 本研究设计并制备了一种聚多巴胺甲基丙烯酸酰胺-聚丙烯酰胺(PDMA-PAAM)水凝胶. 将多巴胺引入到聚丙烯酰胺水凝胶中, 通过多巴胺的氨基与邻苯二酚基团在有机-无机界面上建立共价和非共价相互作用提高了界面粘接力. 金属电极与人体皮肤之间形成了强附着和有效模量过渡体系, PDMA-PAAM水凝胶与猪皮之间的剥离力达到 $22 \text{ N m}^{-1}$ . 此外, 通过添加氯化钠和甘油, PDMA-PAAM水凝胶具有稳定的电导率和室温下60天以上的长期使用寿命. 将本研究制备的PDMA-PAAM水凝胶集成在柔性金电极上用于脑机接口, 采集到的脑电信号强度和波形与同类商用产品基本一致, 且PDMA-PAAM水凝胶柔性电极具有更稳定的界面.